Dalton Transactions

Accepted Manuscript

ROYAL SOCIETY OF CHEMISTRY

www.rsc.org/dalton

Journal Name

RSCPublishing

ARTICLE

Characterization of the Interactions between Substrate, Copper(II) complex and DNA and their Role in Rate Acceleration in DNA-based Asymmetric Catalysis

Cite this: DOI: 10.1039/x0xx00000x

Received 00th January 2012,
Accepted 00th January 2012

DOI: 10.1039/x0xx00000x

www.rsc.org/

Apparao Draksharapu, Arnold J. Boersma, Wesley R. Browne* and Gerard Roelfes*

Interactions of the azachalcone derived substrate **Aza** with copper(II) complexes in the presence and absence of st-DNA were studied in detail by UV/Vis absorption, EPR and Raman and (UV and vis) resonance Raman spectroscopies. The binding of **Aza** to the Lewis acidic copper(II) complexes, which results in activation of the substrate, was established spectroscopically. It was shown that the binding of **Aza** differs between **Cu^{II}dmbpy** and **Cu^{II}terpy**, consistent with the observed differences in catalytic asymmetric Diels-Alder reactions with regard to both the rate and enantiomeric preference. Finally, it was shown that DNA has a major beneficial effect on the binding of **Aza** to the copper(II) complex due to the fact that both bind to the DNA. The result is a high effective molarity of both the copper complexes and the **Aza** substrate, which leads to a significant increase in binding of **Aza** to the copper(II) complex. This effect is the key reason for the observed rate acceleration in catalytic reaction brought about by the presence of DNA.

Introduction

DNA-based asymmetric catalysis is a new concept that is based on a hybrid catalyst formed *in situ* by positioning a catalytically active metal complex in proximity to DNA using non-covalent interactions.[1] The second coordination sphere provided by the DNA plays a crucial role to achieve highly efficient enantioselective copper(II) catalysed reactions. This catalysis concept has proven highly successful in delivering exceptional enantioselective C-C bond forming reactions such as the copper catalysed Diels-Alder reaction,[2] Michael addition[3] and Friedel-Crafts alkylation[4], as well as water addition reactions.[5] Recent studies have shown that this approach can be extended readily to perform catalysis at synthetically relevant scales (gram scale) and that the catalyst solutions can be recycled several times, without loss of activity or enantioselectivity.[6] Often, the role of the DNA was not limited to that of chiral scaffold: in many cases the reactions proved to be considerably faster in the presence of DNA compared to the copper(II) complexes alone.[7,4b,5] This phenomenon of DNA-accelerated catalysis illustrates the power of the second coordination sphere in catalysis. Hence, this system presents an ideal starting point for building the expertise necessary to answer fundamental questions facing second coordination sphere catalysis concepts.

A key challenge is to discriminate spectroscopically between not only bound and unbound catalytic species but also species bound in different environments. Such information is necessary to identify, at a molecular level, the precise mechanism by which the chiral information contained within the structure of DNA is transferred in a highly efficient manner to the product of Lewis acid catalysed reactions, specifically the reactions catalysed by copper(II) and its complexes, and elucidation of the origin of the observed rate accelerating effect of DNA.[7] In answering these general questions, several specific questions need to be addressed including (1) the binding mode of the catalytically active complex to DNA, (2) the interaction of the catalyst with DNA and the changes that occur when substrate is bound, (3) the nature of the microenvironment provided by DNA and (4) the role DNA plays in catalysis. Specifically, which interactions are important in achieving enantioselectivity and reaction rate acceleration.

In the present contribution, a detailed spectroscopic study was performed in order to understand the binding behaviour of the substrate (*E*)-3-(4-methoxyphenyl)-1-(4-methylpyridin-2-yl)prop-2-en-1-one (**Aza**) to Cu-L/DNA, where L are ligands from the second generation, including 4,4'-dimethyl-2,2'-bipyridine (dmbpy), 2,2'-bipyridine (bpy), phenanthroline (phen) and 2,2':6',2''-terpyridine (terpy) (Fig. 1). The

corresponding DNA-based catalysts have been employed successfully in the enantioselective Diels-Alder reaction of azachalcone with cyclopentadiene, resulting in good to excellent ee's.[2a,8] Also a moderate to large rate acceleration was observed in the presence of DNA. Interestingly, in the Diels-Alder reaction between the azachalcone derivative **Aza** and cyclopentadiene, catalysed by **Cu^{II}dmbpy**/DNA or **Cu^{II}terpy**/DNA, the product was obtained with +>99 and -92% ee, respectively.[8] An additional observation is that the reaction rates were found to be much lower with **Cu^{II}terpy** than with **Cu^{II}dmbpy.**

In the preceding contribution in this special issue,[9] we showed that **Cu^{II}dmbpy** and **Cu^{II}bpy** mostly engage in groove binding with DNA, whereas **Cu^{II}phen** and **Cu^{II}terpy** predominantly show intercalative binding. However, it was found that, more that in addition to the DNA binding mode, the flexibility and dynamics of binding are important to achieve high ee's. Here, we focus on understanding the reasons behind the rate enhancements observed in the copper(II) catalysed Diels-Alder reactions brought about by the presence of DNA. The various interactions between the copper(II) ion or Cu^{II}L complex, the **Aza** substrate and salmon testes DNA (st-DNA), are explored by UV/Vis absorption, Raman and EPR spectroscopies. The binding of **Aza** to the copper(II) centre in presence and absence of DNA is studied and a binding geometry is proposed that rationalises the observed differences in enantioselectivity and reactivity between **Cu^{II}(dmbpy)** and **Cu^{II}(terpy)**. Finally, we demonstrate that an increase in local concentration of both complex and substrate in proximity to the DNA is the primary reason for the observed rate enhancement in DNA-based asymmetric catalysis.

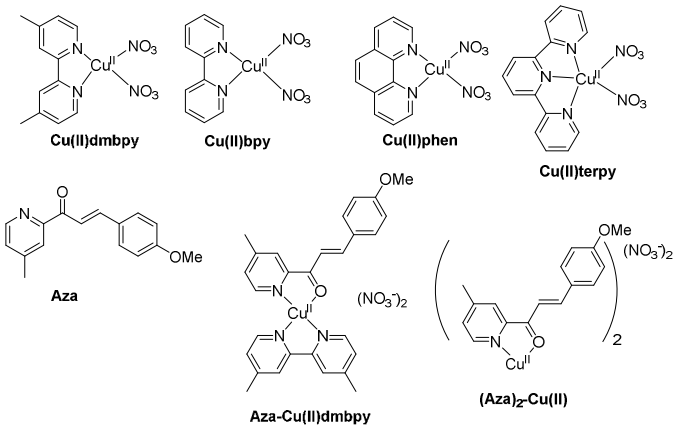

Fig. 1 Structures of the copper(II) complexes and (*E*)-3-(4-methoxyphenyl)-1-(4-methylpyridin-2-yl)prop-2-en-1-one (**Aza**).

Results

The synthesis and characterisation of complexes **Cu^{II}L·(NO$_3$)$_2$** (where L = dmbpy, bpy, phen and terpy, Fig. 1) are described elsewhere.[2a,10] The synthesis of the azachalcone derivative (*E*)-3-(4-methoxyphenyl)-1-(4-methylpyridin-2-yl)prop-2-en-1-one (**Aza**) is given in the experimental section. Elemental analysis indicates the isolation of **(Aza)$_2$-Cu^{II}** from a solution of Cu^{II} and **Aza**, which is supported by UV/Vis absorption, FTIR and Raman spectroscopy. The ternary complex **Aza-Cu^{II}dmbpy** was obtained by slow evaporation of an ethanol solution of Cu(NO$_3$)$_2$, dmbpy and **Aza**, as a green crystalline powder and was characterised by elemental analysis and Raman spectroscopy (*vide infra*). For both complexes, FTIR and Raman spectra confirm complexation through binding by both the pyridine nitrogen and the carbonyl oxygen of **Aza** (Figs. S1 and S2), manifested in a shift to lower wavenumbers for both carbonyl and pyridyl stretching bands and the characteristic bathochromic shift in the lowest absorption band from *ca*. 350 to *ca*. 450 nm due to coordination of a Lewis acid (*i.e.* copper(II)) to the carbonyl. The non-resonant Raman spectra of **Aza-Cu^{II}dmbpy** resembles the spectrum of **(Aza)$_2$-Cu^{II}** with minor shifts in band positions and with additional bands that correspond to the dmbpy ligand (Fig. S2).

Comparison of the Raman spectrum in the solid state and in aqueous acetonitrile solution shows that the **Aza** ligand remains coordinated upon dissolution in the case of **(Aza)$_2$-Cu^{II}** (Fig. S3), but is fully dissociated in the case of **Aza-Cu^{II}dmbpy** (*i.e.*, the spectrum of the latter is a sum of **Cu^{II}dmbpy** and **Aza**, Fig. 2).

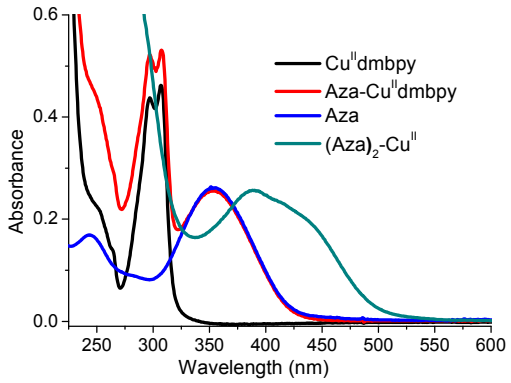

Fig. 2 UV/Vis absorption spectra (0.03 mM) of **Cu^{II}dmbpy**, **Aza-Cu^{II}dmbpy**, **Aza** and **(Aza)$_2$-Cu^{II}** in Milli Q water with 1 vol% acetonitrile.[11]

Evidence for concentration of Aza into st-DNA

The absorption band of **Aza** at 350 nm shows a minor hypochromic change upon addition of st-DNA (Fig S4, inset). Raman spectra recorded at λ_{exc} 355 nm, in resonance with the lowest energy absorption band of **Aza**, showed that the intensity of the band at ca. 1600 cm^{-1} decreases by ca. 75% in the presence of st-DNA (Fig. S4). These changes indicate that interaction between **Aza** and DNA is sufficiently strong to perturb the former's electronic structure and, hence, indicates intercalation between the base pairs.[12] The extent of interaction between **Aza** and st-DNA has consequences with regard to subsequent interaction with copper(II) and its complexes (*vide infra*).

Spectroscopic characterisation of the interactions between Aza, $Cu^{II}(NO_3)_2$ and st-DNA in aqueous solution

Titration of a solution of $Cu(NO_3)_2$ (present in excess) with **Aza** resulted in an increase in absorbance at 350 nm, assigned to uncoordinated **Aza** and at ca. 430 nm, which is consistent with complexation of copper(II) to **Aza** (Fig. 3a). Notably, in the presence of st-DNA, the absorbance at 350 nm is much less, while the absorbance at ca. 430 nm dominates the spectrum (Fig. 3b). These data indicate that the presence of DNA increases the extent copper(II) complexes **Aza** in solution.

Raman spectroscopy at λ_{exc} 355 nm and 473 nm were used to probe the species present in solution, making use of resonance enhancement to observe selectively only those species that show absorbance at the wavelengths employed.[13] The Raman spectrum of st-DNA at either wavelength is unaffected by addition of $Cu(NO_3)_2$. Similarly the Raman spectrum of **Aza** at λ_{exc} 355 nm is relatively unaffected by addition of $Cu(NO_3)_2$, except for a decrease in intensity (Fig. 4), which decreases further in the presence of st-DNA, and in both cases concomitant with the decrease in absorption at that wavelength. The decrease confirms the shift towards coordination of **Aza** by copper(II) in each case.

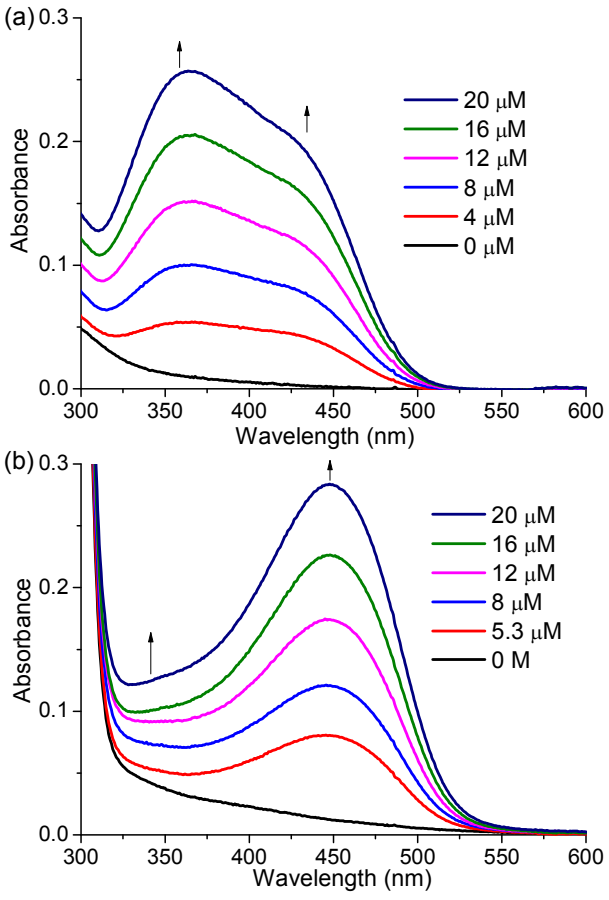

Fig. 3 Titration of (a) **Aza** to $Cu(NO_3)_2$ (0.3 mM) and (b) **Aza** to $Cu(NO_3)_2$ (0.3 mM) with st-DNA (1.33 mg/mL) monitored by UV/Vis absorption spectroscopy (in 20 mM MOPS buffer, pH 6.5). Final concentrations of **Aza** are indicated in the legend.

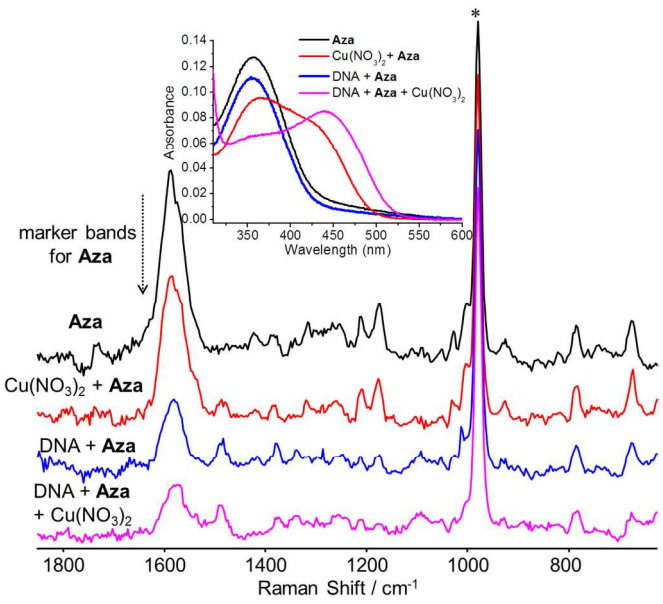

Fig. 4 Resonance Raman spectra of **Aza** (10 μM) and $Cu(NO_3)_2$ (0.3 mM) in the absence and presence of st-DNA (1.33 mg/mL) at λ_{exc} 355 nm in 20 mM MOPS, pH 6.5. * internal standard SO_4^{2-} (50 mM), # acetonitrile bands. Inset: UV/Vis absorption spectra of solutions used to record Raman spectra.

The Raman spectra at λ_{exc} 473 nm, which corresponds to the wavelength at which copper(II) coordinated **Aza** has an absorption band, probe selectively the presence of such species. The Raman spectra of **Aza** with $Cu(NO_3)_2$ both in the absence and presence of st-DNA are similar albeit with minor differences in the wavenumber shifts of certain bands and with an increase in signal intensity in the presence of DNA (Fig. 5), consistent with the increase in absorption observed. The shifts are not monotonic, with bands between 1400 to 1630 cm^{-1} (*i.e.*, C=C and C=N modes) shifted to lower wavenumber and others (1375 cm^{-1}) to higher wavenumber. The band at 1624 cm^{-1}, assigned to a C=O stretch, is also observed in the case with $\mathbf{Cu^{II}dmbpy}$ and $\mathbf{Cu^{II}bpy}$ (*vide infra*). The C=O mode of **Aza** is shifted by -46 cm^{-1} upon coordination to $Cu(NO_3)_2$ as expected for a carbonyl coordinated to a Lewis acid.[14]

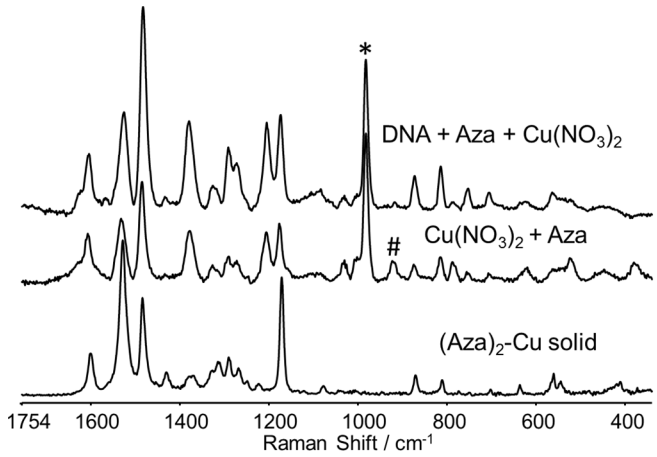

Fig. 5 Resonance Raman spectra of a mixture of $Cu^{II}(NO_3)_2$ (0.3 mM) and **Aza** (10 μM) in 20 mM MOPS buffer in the absence (middle) and presence (top) of st-DNA (1.33 mg/mL) at λ_{exc} 473 nm and solid state Raman spectrum of **$(Aza)_2Cu^{II}$** at λ_{exc} 785 nm. * SO_4^{2-} (50 mM) was used as an internal standard. # acetonitrile band.

Binding of copper(II) complexes and Aza to the st-DNA

The coordination of **Aza** to complexes **Cu^{II}dmbpy**, **Cu^{II}bpy**, **Cu^{II}phen**, **Cu^{II}terpy** and $Cu(NO_3)_2$ was investigated both in the absence and presence of st-DNA by EPR, UV/Vis absorption, Raman and resonance Raman spectroscopy

Interaction of Cu^{II}dmbpy and Aza in the absence and presence of st-DNA

Addition of **Aza** to a solution of $Cu(NO_3)_2$ (*vide supra*) resulted in the appearance of both an absorption band at 350 nm (of **Aza**) and an additional visible absorption band at ca. 430 nm, consistent with binding of **Aza** to a Lewis acid. In contrast, titration of **Aza** to **Cu^{II}dmbpy** in the absence of st-DNA (Fig S5a) resulted in only a monotonic increase in the absorption at 350 nm, *i.e.* of the unbound **Aza** added. In the presence of st-DNA, in contrast, the appearance of a new band at 448 nm was observed upon addition of **Aza** to **Cu^{II}dmbpy** (Fig. S5b).

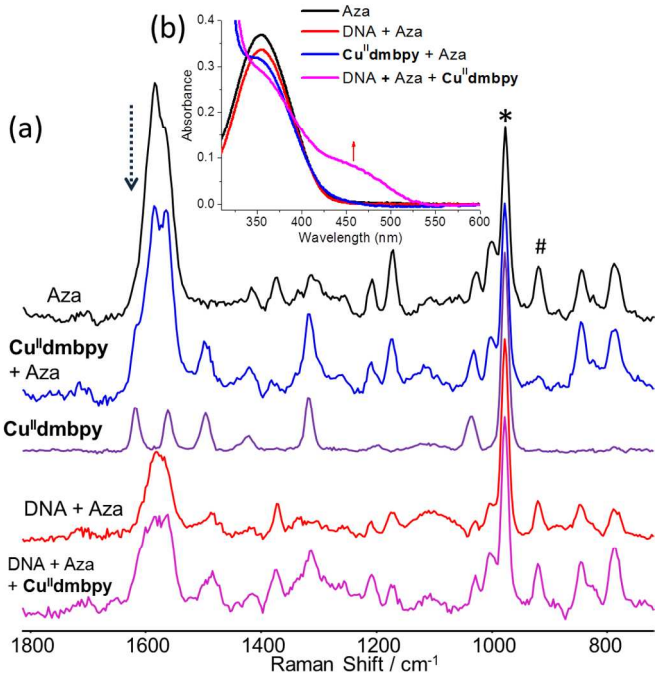

Fig. 6 (a) Resonance Raman spectra at λ_{exc} 355 nm of **Aza** (20 μM) and **Cu^{II}dmbpy** (0.3 mM) in the absence and presence of st-DNA (1.33 mg/mL), in 20 mM MOPS buffer. * internal standard SO_4^{2-} (50 mM), # acetonitrile band and (b) UV/Vis absorption spectra of solutions used to record Raman spectra.

As with $Cu(NO_3)_2$ and **Aza**, resonance Raman spectroscopy at 355 nm and 473 nm allows for identification of both unbound and bound **Aza**, respectively. Furthermore, complexes such as **Cu^{II}dmbpy** show characteristic Raman spectrum at λ_{exc} 355 nm (Fig. 6, see ref 9 for details). As observed by UV/Vis absorption spectroscopy (Fig. 2), addition of **Aza** to an aqueous solution of **Cu^{II}dmbpy** results in a spectrum which is a linear combination of the spectra of each species alone, confirming that little if any coordination of **Aza** to **Cu^{II}dmbpy** occurs. Addition of st-DNA, however, leads to a substantial reduction in the intensity of the **Aza** bands.

The Raman spectra (at λ_{exc} 473 nm) of **Aza** with **Cu^{II}dmbpy** in the absence and presence of st-DNA are shown in Fig. 7. The Raman spectrum of a solution of **Cu^{II}dmbpy** with **Aza** shows resonantly enhanced bands characteristic of both copper(II) coordinated dmbpy and **Aza**. Addition of st-DNA results in a substantial change to the Raman spectrum with an increase in intensity in the Raman bands of over an order of magnitude (consistent with the increase in absorption at 473 nm). Notably, the resonance Raman spectrum of a solution of **DNA** with **Cu^{II}dmbpy** and **Aza** is similar to the solid state spectrum of **Aza-Cu^{II}dmbpy** at 473 nm, albeit with the relative intensities of the bands being somewhat different and the C=O stretch band at 1624 and 1634 cm^{-1}, respectively. The 10 cm^{-1} shift might be due to hydrogen bonding in water as suggested by earlier DFT calculations.[8]

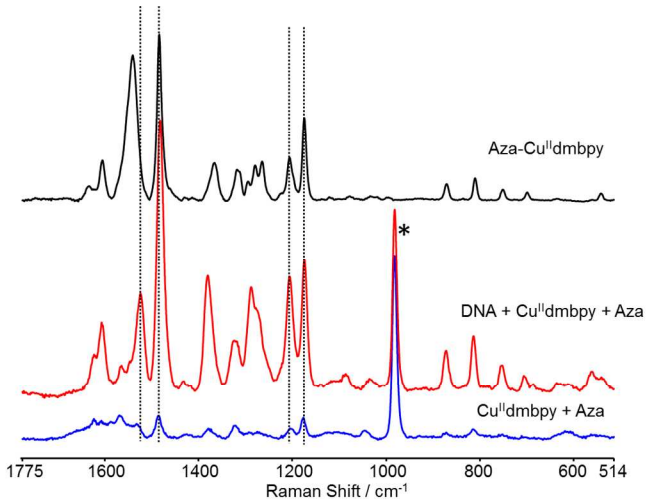

Fig. 7 Raman spectra at λ_{exc} 473 nm of mixture of **Cu^{II}dmbpy** (0.3 mM) and **Aza** (20 µM) in the absence (blue) and presence (red) of st-DNA (1.33 mg/mL) in 20 mM MOPS buffer. The solid state Raman spectrum of **Aza-Cu^{II}dmbpy** dispersed in KCl at λ_{exc} 473 nm is shown (top) for comparison. * internal standard SO_4^{2-} (50 mM). The main characteristic bands of bound **Aza** are indicated with dotted lines.

Contributions from the dmbpy ligand are not readily apparent in the spectrum of the solution containing **DNA** with both **Cu^{II}dmbpy** and **Aza**, which is consistent with the absorption band at 450 nm being predominantly due to a π–π* transition of the **Aza**. Coordination of **dmbpy** to copper(II) under these conditions is confirmed, however, by subtraction of the Raman spectrum with **Cu^{II}d$_{12}$-dmbpy** from that with **Cu^{II}dmbpy** in the presence of st-DNA and **Aza** (Fig. S6) and by Raman spectroscopy at λ_{exc} 355 nm (*vide supra*) and EPR spectroscopy (*vide infra*). Analogous experiments were carried out with the complexes **Cu^{II}bpy, Cu^{II}phen** and **Cu^{II}terpy** (Figs. S7-S12). Addition of **Aza** to st-DNA and complexes **Cu^{II}bpy** and **Cu^{II}phen** results in the appearance of a new absorption at ca. 450 nm albeit less intense that that observed with **Cu^{II}dmbpy**. Furthermore, the resonance Raman spectra at λ_{exc} 473 nm are essentially the same in each case albeit with ca. 50% of the spectral intensity in comparison with **Cu^{II}dmbpy** and with a difference in the weaker bands due to bpy and phen, respectively.

In contrast, a band at 450 nm was not observed with **Cu^{II}terpy** under these conditions and the Raman spectrum at 473 nm was distinctly different to those of the other complexes (Fig. S13), due to the absence of absorbance by copper(II) bound **Aza** and, hence, no resonance enhancement of its Raman scattering.

EPR spectroscopy

The coordination of **Aza** to **Cu^{II}dmbpy** and to **Cu^{II}terpy** was studied by EPR spectroscopy. In contrast to UV/Vis absorption spectroscopy where the intense absorption of **Aza** required analysis under conditions where **Aza** is present in low concentration relative to copper(II) and the copper(II) complexes, much higher concentrations and even excess **Aza** could be employed in EPR spectroscopic studies.

The order $g_{||}>g_{\perp}>2.0023$ of the spectrum of **Cu^{II}dmbpy** indicates axial symmetry with the $d(x^2-y^2)$ orbital as HOMO and a resolved quintet superhyperfine structure ($A_{\perp}$), consistent with coordination by two nitrogen atoms (Fig S14). Addition of up to 3 equiv. of **Aza**[15] to **Cu^{II}dmbpy** led to a decrease in the shift of parallel signals ($g_{||}$), and an increase in the splitting to a heptet ($A_{||}$) with a decrease in the ratio $g_{||}/A_{||}$ (Table S1, Figure S14), consistent with exchange of aqua ligands with **Aza**, which coordinates through a nitrogen and an oxygen atom. Further addition of **Aza** (up to 20 equiv.) resulted in broadening of the signals suggesting the presence of additional species, possibly involving coordination of a second equivalent of **Aza**.

The addition of st-DNA to **Cu^{II}dmbpy** did not change the spectrum substantially except for the appearance of minor additional bands, tentatively assigned to that fraction of complex bound to DNA (Fig S15b).[9] Addition of 1 or more equiv. of **Aza** to **Cu^{II}dmbpy**/st-DNA led to a broadening of the low-field bands and loss of the superhyperfine coupling in the perpendicular direction, consistent with the presence of multiple species, for example *mono* and *bis*-**Aza** complexes of **Cu^{II}dmbpy,** in addition to **Cu^{II}dmbpy** itself.
Based on EPR spectroscopy it can be concluded that at high concentrations **Aza** coordinates to **Cu^{II}dmbpy** via the pyridine nitrogen as well as the carbonyl (as inferred from vibrational spectroscopy, *vide supra*) both in the absence and presence of st-DNA. Furthermore in the presence of st-DNA multiple copper(II) complexes are present, possibly due to different stoichiometries, different geometries, and/or the complexes binding at a range of DNA sites.

Addition of **Aza** to **Cu^{II}terpy** resulted in a shift in the parallel signals to a lower g value (Fig. S16, Table S2). Although the perpendicular superhyperfine coupling was not sufficiently resolved to confirm the number of coordinating nitrogens, with 1 equiv. of **Aza** only two species are apparent in the EPR spectrum, one of which is **Cu^{II}terpy,** while with an excess only the second species is observed. Importantly, there is no evidence for coordination of a second **Aza** ligand. Addition of **Aza** to st-DNA/**Cu^{II}terpy** led to similar changes indicating coordination of one **Aza** ligand to **Cu^{II}terpy** (Fig. S17). In contrast to **Cu^{II}dmbpy** the EPR spectrum of **Cu^{II}terpy** was relatively unaffected by addition of st-DNA.

Discussion

In the present study the interplay between the copper(II) catalysts, **Aza** and DNA was examined through a combination of UV/Vis absorption, resonance Raman and EPR spectroscopies. UV/Vis absorption spectroscopy is particularly suited to determine the extent of complexation of copper(II) to **Aza**, since coordination via the carbonyl oxygen results in a bathochromic shift in the lowest absorption band (from 350 to 450 nm) due to the Lewis acidity of the copper(II) centre. Resonant enhancement of Raman scattering intensity from a species occurs when the wavelength of excitation coincides with an electronic absorption of that species. In the present study excitation at 355 nm and at 473 nm enables quantitative

analysis of, in particular **Aza**, species in solution under various conditions.

The coordination of **Aza** to copper(II) was found to be favourable in the absence of polypyridyl ligands. Indeed both UV/Vis absorption and Raman spectroscopy indicated that the complexes **$(Aza)_2$-Cu^{II}** and **Aza-Cu^{II}** are relatively stable in aqueous solution even at low concentration. Nevertheless the shift towards Cu^{II} bound **Aza** observed in the presence of st-DNA is readily apparent, raising an important question as to the latter's role. Indeed, it should be noted that in certain cases[2a] $Cu^{II}(NO_3)_2$ with DNA catalysed Diels-Alder reactions with modest enantioselectivity, indicating that Cu^{II} salts and the complexes formed with **Aza** associate relatively strongly with DNA, which might be driven both by electrostatic interactions and groove binding/intercalation. In the present study, the interaction of **Aza** with DNA was manifested in a minor hypsochromic effect. Furthermore, the effect the presence of DNA has on the extent of resonance enhancement of the Raman scattering of **Aza** indicates that it undergoes, most likely, intercalation between the base pairs of DNA. The binding of **Aza** to DNA holds consequences in regard to the Cu^{II} catalysed reactions carried out with it. The binding of both Cu^{II} and **Aza** results in a substantial increase in effective molarity, and thereby increases the proportion of **Aza** bound Cu^{II}. An increase in the effective concentration of the **Aza-Cu^{II}** complex will increase also the rate of reaction under catalytic conditions. This is comparable to the effects observed in Lewis acid catalysis in micellar systems.[16] In the case of $Cu^{II}(NO_3)_2$, the increase in rate will be limited by the fact that the affinity of **Aza** for $Cu^{II}(NO_3)_2$ is already relatively high.

In contrast to $Cu^{II}(NO_3)_2$, it is apparent from UV/Vis absorption and resonance Raman spectroscopy that the binding affinity of the complexes **Cu^{II}L** (where L = dmbpy, bpy, phen and terpy) for **Aza** is low in aqueous solution, as exemplified by the instability of the ternary complex **Aza-Cu^{II}dmbpy** in solution (Fig. 2). The effect of DNA on the binding between **Cu^{II}L** and **Aza** is apparent where L is dmbpy, bpy or phen, from the appearance of the characteristic absorption band at ca. 450 nm. As with $Cu^{II}(NO_3)_2$, the origin of the increase in binding affinity caused by the presence of DNA is most likely due to the increase in effective molarity that the affinity of both the **Cu^{II}L** complexes and **Aza** for DNA causes. This relatively simple effect has an important consequence with regard to catalysis as it accounts, at least to a some extent, for the rate enhancement observed in the presence of DNA observed with **Cu^{II}L** complexes.[7] The extent to which an increase in local concentration can affect reaction rate, however, may also be influenced by the binding mode of the complexes to DNA. The extended conjugation of **Aza** favours adoption of a flat conformation, which would be expected to bind to DNA by intercalation. That this indeed occurs is suggested by the hypochromism and the decrease in the intensity of Raman scattering of **Aza** observed in the presence of DNA. Furthermore, in order to undergo reactions, *e.g.*, the Diels-Alder reaction, the **Aza** needs to de-intercalate and bind to the copper(II) complexes. Complexes, which themselves intercalate, would be expected therefore to both compete with **Aza** for binding sites in the DNA but also bind to **Aza** less easily. By contrast complexes which undergo groove binding and are relatively mobile despite being associated to the DNA will be expected to benefit most from the increased local concentration of **Aza**. Indeed, the equilibrium is shifted towards the **Aza** bound copper(II) complexes in the presence of DNA to a greater extent for **Cu^{II}dmbpy** than for **Cu^{II}bpy** and **Cu^{II}phen**.

The nature of the interaction between the **Cu^{II}L** complexes with DNA was discussed in depth previously.[9] The association of the complexes with DNA was found to be predominately groove binding with intercalation of increasing importance in the order dmbpy, bpy, terpy and phen.

For **Cu^{II}terpy**, UV/Vis absorption spectroscopy indicates that binding to **Aza** does not occur to a significant extent, however, the expected bathochromic shift of the **Aza** absorption is dependent on the coordination of the carbonyl oxygen of the **Aza** to the copper(II) centre. In the case of **Cu^{II}terpy**, which contains the tridentate ligand terpy, EPR spectroscopy indicates that coordination of **Aza** is through the pyridine only and despite the lack of visible absorbance, in fact, occurs to a substantial extent (Fig. 8).

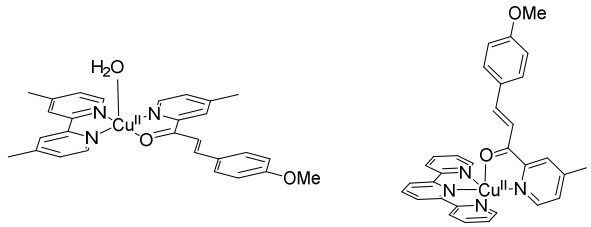

Fig. 8 Proposed coordination modes of **Aza** to **Cu^{II}dmbpy** and **Cu^{II}terpy**.

Similar geometries have been proposed for other ternary complexes based on Cu^{II}/2,2'-bipyridine and Cu^{II}/2,6-terpyridine.[17,18] According to the proposed coordination modes of **Aza**, the substrate is required to bind in a bidentate fashion, which has been argued before on the basis of substrate variation.[19] Indeed, in the case of **Cu^{II}dmbpy**, **Aza** was calculated to coordinate in a bidentate fashion in the pseudo-equitorial plane via the carbonyl oxygen and pyridine nitrogen. In the case of **Cu^{II}terpy** it was shown that **Aza** coordinates via the pyridine nitrogen, and the carbonyl oxygen, in order to lower the LUMO. The conversions of the reactions catalysed by **Cu^{II}terpy**/DNA were found to be lower compared to **Cu^{II}dmbpy**/st-DNA.[8] This is expected if the carbonyl is coordinated axially, which is also suggested by DFT calculations,[8] since the axial bond to copper(II) is elongated considering the axial symmetry obtained from EPR.

Another consequence of the proposed structures is that **Cu^{II}terpy** is coordinatively saturated upon binding of a single **Aza** ligand, as noted by EPR spectroscopy (*vide supra*). By contrast, for **Cu^{II}dmbpy** in the presence of excess **Aza**, EPR spectroscopy suggests that an **$(Aza)_2$-Cu^{II}dmbpy** complex forms also.

The structure of **Aza-Cu^{II}terpy** apparently does not change upon addition of st-DNA. On the other hand, in the case of **Aza-Cu^{II}dmbpy** changes are observed due to the presence of st-DNA. In EPR multiple copper(II) species appeared upon addition of st-DNA. This can be rationalized by small variations in the coordination geometry, replacement of coordinated water by a coordinating group of st-DNA, or even the formation of diastereomeric complexes.[20]

Conclusions

We have established spectroscopically the binding of the substrate **Aza** to the Lewis acidic copper(II) complexes, which results in activation of the substrate. It was shown that the binding of **Aza** differs between **Cu^{II}dmbpy** and **Cu^{II}terpy**, which is consistent with the observed differences in catalysis with regard to both the rate and enantiomeric preference of the reaction. Finally, it was shown that DNA has a major beneficial effect on the binding of **Aza** to the copper(II) centre. This is due to the fact that, in addition to the copper(II) complex, **Aza** itself binds to the DNA in a predominantly intercalative fashion. The result is a high effective molarity of both the copper complexes and the **Aza** substrate, which leads to a significant increase in binding of **Aza** to the copper(II) complex. This effect is the key reason for the observed rate acceleration in catalysis brought about by the DNA. However, binding can only occur when **Aza** and the copper(II) complex encounter each other, which requires a dynamic binding of at least one of the binding partners. For this reason, the DNA-induced rate acceleration in catalysis was observed with **Cu^{II}dmbpy**, which was shown to bind dynamically in the DNA grooves. Indeed, **Cu^{II}phen** and **Cu^{II}terpy**, which bind in a more static, intercalative fashion, show much lower DNA induced acceleration in catalysis.

In conclusion, this study shows unequivocally that DNA-based catalysts successfully balance the chiral interactions required for high enantioselectivity with enough dynamics to achieve high rate accelerations in catalysis. Thus, these findings underline the power of the second coordination sphere concept in catalysis.

Experimental section

Synthesis

Salmon testes DNA (st-DNA) was obtained from Sigma Aldrich. st-DNA was dialyzed extensively against MOPS buffer (20 mM, pH 6.5) prior to use. The complexes [Cu(dmbpy)(NO$_3$)$_2$] (**Cu^{II}dmbpy**),[2a] [Cu(d$_{12}$-dmbpy)(NO$_3$)$_2$] (**Cu^{II}d$_{12}$-dmbpy**), [Cu(bpy)(NO$_3$)$_2$] (**Cu^{II}bpy**),[2a] [Cu(phen)(NO$_3$)$_2$] (**Cu^{II}phen**)[2a] and [Cu(terpy)(NO$_3$)$_2$] (**Cu^{II}terpy**)[9] and (*E*)-3-(4-methoxyphenyl)-1-(4-methylpyridin-2-yl)prop-2-en-1-one (**Aza**)[8] were prepared and isolated as previously reported. d$_{12}$-dimethylbipyridine (d$_{12}$-dmbpy) was prepared as reported previously.[21] Commercially available chemicals were used without further purification unless stated otherwise. Solvents for spectroscopic measurements were UVASOL (Merck) grade or better. For titrations, an equilibration time of ca. 1 min was used, however, significant further changes were not observed even after several hours. Unless stated otherwise all solutions were adjusted to pH 6.5 for direct comparison with catalytic conditions employed earlier.[5-8]

(Aza)$_2$-Cu^{II}(NO$_3$)$_2$.2H$_2$O. Cu(NO$_3$)$_2$.3H$_2$O (20 mg, 0.027 mmol) solid was added to a acetonitrile solution (1 mL) of **Aza** (20.5 mg, 0.08 mmol). The resulting yellowish brown solid was filtered and dried over air and the solid **Aza-Cu** was characterized by UV/Vis absorption, IR and Raman spectroscopy. Elemental analysis indicates a composition of (Aza)$_2$Cu^{II}(NO$_3$)$_2$·2H$_2$O. Anal. Cald. C, 52.5 H, 4.78 N, 7.65. Found C, 52.4 H, 4.22 N, 7.70.

[(dmbpy)Cu(Aza)](NO$_3$)$_2$.½H$_2$O] (Aza-Cu^{II}dmbpy). A solution of 4,4'-dimethyl-2,2'-dipyridyl (57 mg, 0.31 mmol) in a minimal amount of EtOH was added to a solution of Cu(NO$_3$)$_2$.3H$_2$O (75 mg, 31 mmol) in a minimum amount of EtOH. **Aza** (75 mg, 30 mmol) in a minimum amount of EtOH was added dropwise to the mixture. The dark green solution was passed over a cotton plug in order to remove the brown precipitate that formed. The filtrate was evaporated slowly over 24 h to yield a green micro crystalline powder, which was recovered by filtration and washed with EtOH. Anal. Cald for C$_{28}$H$_{27}$CuN$_5$O$_8$.½H$_2$O: C, 53.0 H, 4.45 N, 11.04. Found: C, 52.8 H, 4.39 N, 11.19.

Physical Methods

Elemental analyses were performed with a Foss-Heraeus CHN Rapid or a EuroVector Euro EA elemental analyzer. ^{1}H NMR spectra (400 MHz) were recorded on a Varian Mercury Plus. Chemical shifts are denoted relative to the residual solvent peak (^{1}H NMR spectra CD$_3$Cl, 7.26 ppm). EPR spectra (X-band, 9.46 GHz) were recorded on a Bruker ECS106 spectrometer in liquid nitrogen (77 K). UV/Vis absorption spectra were recorded with a Specord600 (AnalytikJena) spectrophotometer in 1 cm path length quartz cuvettes. FTIR spectra were recorded using a UATR (ZnSe) with a Perkin Elmer Spectrum400, equipped with a liquid nitrogen cooled MCT detector. Raman spectra were obtained in an 135° backscattering arrangement with excitation at 355 nm (10 mW, Cobolt Lasers) and 473 nm (100 mW, Cobolt Lasers) with Raman scattering collected and collimated (f = 7.5 cm) and subsequently refocused (f = 7.5 cm and 17.5 cm) via a pair of 2.5 cm diameter plano-convex lens. The collected light was filtered by an appropriate long pass edge filter (Semrock) and dispersed by a Shamrock300i or 500i spectrograph (Andor Technology) with a 1200 l/mm grating blazed at 500 nm, or 2400 l/mm blazed at 300 nm and acquired with a DV420A-BU2 CCD camera (Andor Technology). The slit width was set to 60 μm. Data were recorded and processed using Solis (Andor Technology) with spectral calibration performed using the Raman spectrum of cyclohexane or acetonitrile/toluene 50:50 (v:v). Samples were held in quartz 10 mm path length cuvettes.

Solvent subtraction and a multipoint baseline correction were performed for all spectra. Raman spectra were recorded at λ_{exc} 785 nm using a Perkin Elmer Raman Station at room temperature. KCl dispersed Cu complexes were prepared by crushing the desired Cu complex with KCl in a mortar.

Acknowledgements

Financial support is acknowledged from the European Research Council (ERC consolidator grant 279549, WRB), the Ubbo Emmius Fund of the University of Groningen (AD), the National Research School Catalysis (AB, GR) and from the Ministry of Education, Culture and Science (Gravity program 024.001.035, GR WRB).

Notes and references

Stratingh Institute for Chemistry, Faculty of Mathematics and Natural Sciences, University of Groningen, Nijenborgh 4, 9747AG, Groningen, The Netherlands. j.g.roelfes@rug.nl, w.r.browne@rug.nl, tel. +31-50-363-4428

† Electronic Supplementary Information (ESI) available: Details of synthesis and characterization of deuterated ligands and complexes, additional spectroscopic data. See DOI: 10.1039/b000000x/

1 A. J. Boersma, R. P. Megens, B. L. Feringa and G. Roelfes, *Chem. Soc. Rev.*, 2010, **39**, 2083; (b) S. Park and H. Sugiyama, *Angew. Chem., Int. Ed.*, 2010, **49**, 3870; (c) J. Oelerich and G. Roelfes, 'DNA-Based Metal Catalysis', in *Progress in Inorganic Chemistry*, *vol 57*, K.D. Karlin (Ed.), John Wiley & Sons, Inc., Hoboken, New Jersey, **2012**, pp. 353-393.

2 (a) G. Roelfes, A. J. Boersma and Feringa, B. L., *Chem. Commun.*, 2006, 635; (b) S. Roe, D. J. Ritson, T. Garner, M. Searle and J. E. Moses, *Chem. Commun.*, 2010, **46**, 4309; (c) J. Wang, E. Benedetti, L. Bethge, S. Vonhoff, S. Klussmann, J. Vasseur, J. Cossy, M. Smietana, S. Arseniyadis, *Angew. Chem., Int. Ed.*, 2013, **52**, 11546.

3 (a) D. Coquière, B. L. Feringa and G. Roelfes, *Angew. Chem., Int. Ed.*, 2007, **46**, 9308; (b) Y. Li, C. Wang, G. Jia, S. Lu, C. Li, *Tetrahedron, 2013*, **69**, 6585.

4 (a) S. Park, K. Ikehata, R. Watabe, Y. Hidaka, A. Rajendran and H. Sugiyama, *Chem. Commun.*, 2012, **48**, 10398; (b) A. J. Boersma, B. L. Feringa and G. Roelfes, *Angew. Chem., Int. Ed.*, 2009, **48**, 3346.

5 A. J. Boersma, D. Coquière, D. Geerdink, F. Rosati, B. L. Feringa and G. Roelfes, *Nat. Chem.*, 2010, **2**, 991.

6 R. P. Megens and G. Roelfes, *Org. Biomol. Chem.*, 2010, **8**, 1387.

7 A. J. Boersma, J. E. Klijn, B. L. Feringa and G. Roelfes, *J. Am. Chem. Soc.*, 2008, **130**, 11783.

8 A. J. Boersma, B. de Bruin, B. L. Feringa and G. Roelfes, *Chem. Commun.*, 2012, **48**, 2394.

9 A. Draksharapu, A. J. Boersma, M. Leising, A. Meetsma, W. R. Browne and G. Roelfes, *Dalton trans.*, 2014 (submitted).

10 M. Navarro, E. J. Cisneros-Fajardo, A. Sierralta, M. Fernandez-Mestre, P. Silva, D. Arrieche and E. Marchan, *J. Biol. Inorg. Chem.*, 2003, **8**, 401.

11 MilliQ water was employed to exclude coordination of buffer components to the copper complexes.

12 C. A. Butler, R. P. Cooney and W. A. Denny, *Appl. Spectr.* 1994, **48**, 822

13 W. R. Browne and J. J. McGarvey, *Coord. Chem. Rev.*, 2007, **251**, 454.

14 M. F. Lappert, *J. Chem. Soc.*, 1962, 542; (b) C. S. Branch, S. G. Bott and A. R. Barron, *J. Organomet. Chem.*, 2003, **23**, 666.

15 Due to the low solubility of **Aza** in water a mixture of MOPS buffer and ethanol (1:2, v/v) was used.

16 (a) S. Otto, J. B. F. N. Engberts and C. T. kwak, *J. Am. Chem. Soc.*, 1998, **120**, 9517; (b) F. Rosati, J. Oelerich and G. Roelfes, *Chem. Commun.*, 2010, 7804.

17 S. Suzuki, T. Sakurai, S. Itoh and Y. Ohshiro, *Inorg. Chem.*, 1988, **27**, 591.

18 T. Kohzuma, A. Odani, Y. Morita, M. Takani and O. Yamauchi, *Inorg. Chem.*, 1988, **27**, 3854.

19 S. Otto, F. Bertoncin and J. B. F. N. Engberts, *J. Am. Chem. Soc.*, 1996, **118**, 7702.

20 Since **Aza-Cu(II)dmbpy** is not perfectly square planar, due to repulsion of the 3 and 3' hydrogens, it is very likely that the complex adopts a helical conformation. If **Aza** would coordinate in a square pyrimidal fashion, the complex is chiral also.

21 W. R. Browne, C. M. O'Connor, J. S. Killeen, A. L. Guckian, M. Burke, P. James, M. Burke and J. G. Vos, *Inorg. Chem.*, 2002, **41**, 4245.

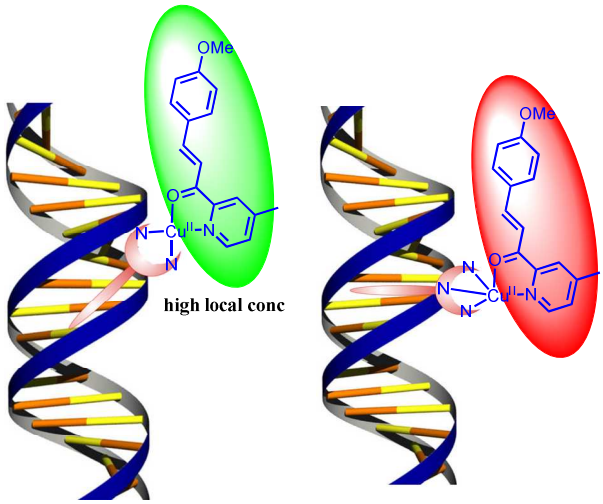

High effective molarity is responsible for the significant increase of binding of substrates to copper(II) complexes in DNA-based catalysis